5,5-Diethylbarbiturato complexes of copper(II) with (2-aminoethyl)piperidine, -pyrrolidine, and -morpholine: syntheses, crystal structures, spectroscopic, and thermal properties

M. Suat Aksoy[a]; Veysel T. Yilmaz[a]; Orhan Buyukgungor[b]

[a] Faculty of Arts and Sciences, Department of Chemistry, Uludag University, 16059 Bursa, Turkey [b] Faculty of Arts and Sciences, Department of Physics, Ondokuz Mayis University, 55139 Samsun, Turkey

PLEASE SCROLL DOWN FOR ARTICLE

Taylor & Francis
Taylor & Francis Group

5,5-Diethylbarbiturato complexes of copper(II) with (2-aminoethyl)piperidine, -pyrrolidine, and -morpholine: syntheses, crystal structures, spectroscopic, and thermal properties

M. SUAT AKSOY†, VEYSEL T. YILMAZ*† and
ORHAN BUYUKGUNGOR‡

†Faculty of Arts and Sciences, Department of Chemistry,
Uludag University, 16059 Bursa, Turkey
‡Faculty of Arts and Sciences, Department of Physics,
Ondokuz Mayis University, 55139 Samsun, Turkey

Three new complexes, $[Cu(barb)_2(aepip)] \cdot 0.5H_2O$ (**1**), $[Cu(barb)_2(aepyrd)]$ (**2**), and $[Cu(barb)_2(aemrph)]$ (**3**), have been synthesized by reaction of 5,5-diethlybarbiturate anion (barb) with copper(II) in the presence of (2-aminoethyl)piperidine (aepip), -pyrrolidine (aepyrd), and -morpholine (aemrph). All complexes were characterized by elemental analysis, spectroscopic (IR and UV/Vis), thermal (DTA-TGA), and magnetic susceptibility measurements. X-ray single crystal diffraction shows that **1** and **2** are discrete mononuclear species, in which copper(II) is coordinated by two bidentate barb ligands and a chelating aepip or aepyrd, forming a square-pyramidal coordination geometry. Complexes **1** and **2** show unequal coordination of barb, one N-coordinate, and one bidentate. Complex **3** is also mononuclear, but copper(II) is square-planar with two N-coordinated barb and one bidentate aemorph. Molecules of **1**–**3** are bridged by strong hydrogen bonds to generate 1-D or 2-D supramolecular networks. Spectral and thermal data for **1**–**3** are in agreement with crystal structures.

Keywords: 5,5-Diethylbarbiturate; (2-Aminoethyl)piperidine; (2-Aminoethyl)pyrrolidine; (2-Aminoethyl)morpholine; Copper(II)

1. Introduction

Metal complexes of biologically important ligands have interest to the development of new metal-based chemotherapeutic agents. Barbiturates are one such class of biologically active compounds, acting as central nervous system depressants or sedative-hypnotics. Coordination chemistry of barbiturates is important in detection and identification of barbiturate drugs. Levi and Hubley [1] studied reaction of 12 different clinically important barbiturates with copper(II) in the presence of pyridine (py) and suggested the mode of coordination of these barbiturate ligands on the basis of IR spectral data.

*Corresponding author. Email: vtyilmaz@uludag.edu.tr

The presence of several potential donors such as two amine nitrogens and three carbonyl oxygens makes barbiturates interesting polyfunctional ligands. Barbiturates usually coordinate monodentate through deprotonated nitrogens [2–6], but in some cases, the carbonyl oxygens [7, 8] and carbons [8, 9] are involved in coordination depending on the type of metal.

Recently, we have started a research project on the synthesis and characterization of metal complexes of 5,5-diethylbarbituric acid (barbH), also known as barbital or veronal. We found that barb in *cis*-[Cu(barb)$_2$(en)] and {[Cd(barb)$_2$(μ-en)] $\cdot$ 2H$_2$O}$_n$ are bidentate chelating via the negatively charged nitrogen and carbonyl oxygen [10], while in Na$_3$[Ag$_3$ μ-barb)$_6$] and {[Ag$_2$ μ-barb)$_2$][Ag$_2$ μ-en)$_2$] $\cdot$ 5H$_2$O}$_n$ as bridging ligands [11]. This article reports the synthesis and characterization of three new 5,5-diethylbarbiturato complexes of copper(II) with (2-aminoethyl)piperidine (aepip), -pyrrolidine (aepyrd), and -morpholine (aemrph), [Cu(barb)$_2$(aepip)] $\cdot$ 0.5H$_2$O (**1**), [Cu(barb)$_2$(aepyrd)] (**2**), and [Cu(barb)$_2$(aemrph)] (**3**). Spectroscopic properties and thermal behaviors of these complexes are discussed and different coordination modes of barb are established by single-crystal X-ray diffraction studies.

2. Experimental

2.1. *Materials and measurements*

All commercial reagents were used as supplied. Elemental analyses for C, H, and N were performed using a Costech elemental analyzer. IR spectra were recorded with a Thermo Nicolet 6700 FT-IR spectrophotometer with KBr pellets from 4000–400 cm^{-1}. Electronic spectra were measured on a Shimadzu UV-2100 in the 200–900 nm range. Room temperature magnetic susceptibility measurements were carried out using a Sherwood Scientific MXI model Evans magnetic balance. Thermal analysis curves (TGA and DTA) were obtained using a Seiko Exstar 6200 thermal analyzer in a dynamic air atmosphere with a heating rate of 10°C min^{-1} and a sample size of *ca* 10 mg.

2.2. *Synthesis of copper(II) complexes*

Complexes **1**–**3** were prepared using the same synthesis procedure. A solution of Na(barb) (5,5-diethylbarbituric acid sodium salt) (0.206 g, 1 mmol) in distilled water (10 mL) was mixed with a 10 mL aqueous solution of CuSO$_4$ $\cdot$ 5H$_2$O (0.5 mmol, 0.125 g) with stirring. To this solution 10 mL EtOH was added and 0.5 mmol (2-aminoethyl) piperidine (aepip) was added dropwise. The same procedure was repeated for (2-aminoethyl)pyrrolidine (aepyrd) and (2-aminoethyl)morpholine (aemrph). The reaction mixtures were stirred for 30 min at room temperature and the resulting solutions were allowed to stand at room temperature. X-ray quality dark blue prisms of **1**–**3** were formed after 3 days.

[Cu(barb)$_2$(aepip)] $\cdot$ 0.5H$_2$O (**1**): Yield 68%, m.p. 184°C. Anal. Calcd for C$_{23}$H$_{40}$N$_6$O$_{6.5}$Cu (%): C, 48.62; H, 7.09; N, 14.79. Found(%): C, 48.47; H, 7.25; N, 14.53. (Solid KBr pellet): ν (cm^{-1}) 3542sb, 3503sb, 3325m, 3250sb, 3175sb, 3072m,

2969m, 2878w, 1710vs, 1671vs, 1615vs, 1458sh, 1442s, 1417vs, 1370vs, 1317vs, 1257s, 1164w, 1122m, 1037m, 988m, 948w, 860w, 758w, 692w, 630w, 540m, 494w.

[Cu(barb)$_2$(aepyrd)] (**2**): Yield 70%, m.p. 186°C. Anal. Calcd for C$_{22}$H$_{36}$N$_6$O$_6$Cu (%): C, 48.56; H, 6.67; N, 11.68. Found(%): C, 48.73; H, 6.88; N, 11.41. IR (solid KBr pellet): ν (cm^{-1}) 3456sb, 3346vw, 3246sb, 3166sb, 3073w, 2969m, 2936w, 2880w, 1710vs, 1671vs, 1617vs, 1458sh, 1438sh, 1418vs, 1368vs, 1317vs, 1256s, 1165w, 1134w, 1096m, 947m, 823w, 759w, 692w, 540m, 497w, 464w.

[Cu(barb)$_2$(aemrph)] (**3**): Yield 69%, m.p. 197°C. Anal. Calcd for C$_{22}$H$_{36}$N$_6$O$_7$Cu (%): C, 47.18; H, 6.48; N, 11.35. Found(%): C, 46.95; H, 6.71; N, 11.56. (Solid KBr pellet): ν (cm^{-1}) 3449sb, 3343m, 3256s, 3179sb, 3073m, 2969m, 2934w, 2879w, 1711vs, 1671vs, 1616vs, 1459sh, 1418vs, 1364vs, 1318vs, 1255vs, 1118s, 1090s, 1005m, 950w, 923m, 760w, 693w, 628w, 543m, 608s, 444w.

2.3. *X-ray crystallography*

The intensity data of **1**–**3** were collected using a STOE IPDS 2 diffractometer with graphite-monochromated Mo-Kα radiation ($\lambda = 0.71073$) at 296 K. The structures were solved by direct methods and refined on F^2 with the SHELXL-97 program [12]. All nonhydrogen atoms were found from difference Fourier map and refined anisotropically. All hydrogens were included using a riding model. Some C atoms of the ethyl groups of barb were severely disordered over two positions with approximately equal occupancy; the disorder results in short C–C distances and irrelevant intra- or intermolecular interactions. The details of data collection, refinement, and crystallographic data are summarized in table 1.

3. Results and discussion

3.1. *Synthesis and characterization*

Complexes **1**–**3** were obtained by reaction of Na(barb) with CuSO$_4 \cdot$5H$_2$O in the presence of aepip, aepyrd, and aemrph in high yields (around 70%). Analytical data (C, H, and N contents) are consistent with the proposed empirical formulas, also confirmed by single crystal X-ray analysis. Complexes **1**, **2**, and **3** melt at 184, 186, and 198°C, respectively. All three complexes are air stable and highly soluble in warm water and ethanol.

IR spectra of **1**–**3** were recorded in KBr from 4000–400 cm^{-1}; selected spectral data are summarized in table 2. For comparative purposes the IR spectra of the free ligands were also obtained. A remarkable difference between IR spectra of the ligands and those of the corresponding complexes is that the NH vibrations shift to lower frequencies in spectra of all the complexes. Absorption bands of NH$_2$ of the diamine ligands are at higher frequencies than those of barb. Strong and broad absorptions between 3246 and 3346 cm^{-1} indicate the presence of NH groups of the diamine ligands, while bands around 3170 cm^{-1} are assigned to NH of barb. Additionally, broad and strong bands at 3542 and 3503 cm^{-1} correspond to O–H vibrations of lattice water in **1**. Several weak or medium bands were observed in the

Table 1. Crystallographic data and structure refinement for **1**–**3**.

	1	**2**	**3**
Empirical formula	$C_{23}H_{40}N_6O_{6.5}Cu$	$C_{22}H_{36}N_6O_6Cu$	$C_{22}H_{36}N_6O_7Cu$
Formula mass	568.14	544.11	560.11
Crystal system	Monoclinic	Triclinic	Triclinic
Space group	$C2/c$	$P\bar{1}$	$P\bar{1}$
Unit cell dimensions (Å, °)			
a	11.4039(3)	10.6868(7)	10.6045(6)
b	18.0687(6)	10.7875(7)	10.7487(6)
c	26.8949(8)	13.3615(8)	13.9843(8)
α	90.00	99.503(5)	100.372(4)
β	100.392(2)	100.245(4)	104.716(5)
γ	90.00	116.949(5)	117.236(4)
V (Å^3)	5450.9(3)	1297.1(2)	1286.84(15)
Z	4	2	2
D_c (g cm^{-3})	1.382	1.393	1.446
μ (mm^{-1})	1.108	2.428	0.902
$F(000)$	2400	574	590
Crystal size (mm^3)	$0.58 \times 0.36 \times 0.16$	$0.49 \times 0.42 \times 0.24$	$0.42 \times 0.38 \times 0.05$
θ range (°)	2.14–26.50	1.61–26.50	1.60–26.50
Index range (h, k, l)	$-14/14, -22/22, -27/33$	$-13/13, -13/13, -16/16$	$-13/13, -13/13, -17/17$
Reflections collected	15,884	23,141	14,341
Reflections independent	5627 ($R_{int} = 0.0559$)	5367 ($R_{int} = 0.0542$)	5345 ($R_{int} = 0.0662$)
Absorption correction	Numerical	Numerical	Numerical
Data/parameters	5627/345	5367/329	5345/331
Goodness-of-fit on F^2	1.087	1.064	1.043
Final R indices [$I > 2\sigma(I)$]	0.0589	0.0564	0.0508
$\Delta\rho_{max./min.}$ (e Å^{-3})	0.913/$-$0.578	1.142/$-$0.752	0.691/$-$0.505

Table 2. Selected IR spectral data for **1**–**3**.[a]

Assignments	**1**	**2**	**3**
ν(OH)	3542sb, 3503sb	–	–
ν(NH)amine	3325m, 3250sb	3346vw, 3246sb	3343m, 3256s
ν(NH)barb	3175sb	3166sb	3179sb
ν(CH)	3072–2878m, w	3073–2880m, w	3073–2879m, w
ν(CO)	1710vs, 1671vs, 1615vs	1710vs, 1671vs, 1617vs	1711vs, 1671vs, 1616vs
ν_s(CN)	1257s	1256s	1255vs

[a]Frequencies in cm^{-1}; b = broad; w = weak; vs = very strong; s = strong; m = medium.

2980–3075 cm^{-1} range due to C–H stretches. All three complexes displayed three sharp absorptions at 1615, 1671, and 1710 cm^{-1}, for carbonyl of barb, involved in coordination or strong hydrogen bonding. Strong bands from 1460 to 1360 cm^{-1} are skeleton vibrations of the heterocycles and C–H deformation vibrations, while bands from 1256 to 923 cm^{-1} are assigned to ν(C–N) and ν(C–C), and weak bands at 860–628 cm^{-1} are γ(C–H) vibrations.

The electronic spectrum of aqueous solutions of **1**–**3** show broad absorption bands at 637 nm ($\varepsilon = 186$ dm^3 mol^{-1} cm^{-1}) for **1**, 637 nm ($\varepsilon = 189$ dm^3 mol^{-1} cm^{-1}) for **2**, and at 643 nm ($\varepsilon = 175$ dm^3 mol^{-1} cm^{-1}) for **3**. Absorption bands below 300 nm are due to intra-ligand transitions of both barb and diamine ligands.

Room-temperature magnetic susceptibility measurements show the mononuclear complexes are paramagnetic with a μ_{eff} of 1.65, 1.65, and 1.64 BM for **1**, **2**, and **3**,
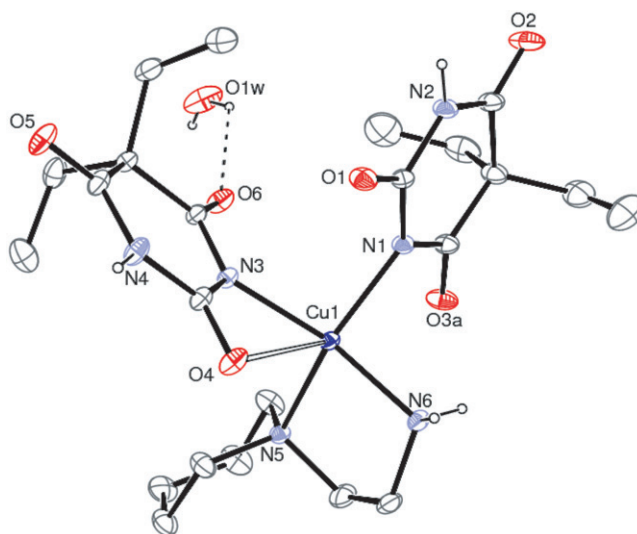
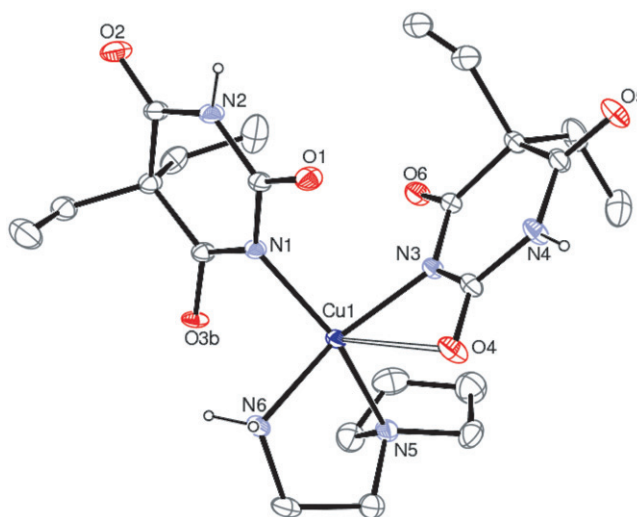Figure 1.   A molecular view of **1** (C–H hydrogens were omitted for clarity).

Figure 2.   A molecular view of **2** (C–H hydrogens were omitted for clarity).

respectively, in satisfactory agreement with the expected μ_{eff} of 1.73 BM for a spin-only d^9 system.

3.2. *Crystal structures*

Molecular structures of **1**–**3** with the atom labeling are shown in figures 1–3 and selected bond lengths and angles together with hydrogen bonding geometry are listed in tables 3–5. The structures of **1**–**3** consist of discrete molecules. Copper(II) in **1** and **2** are
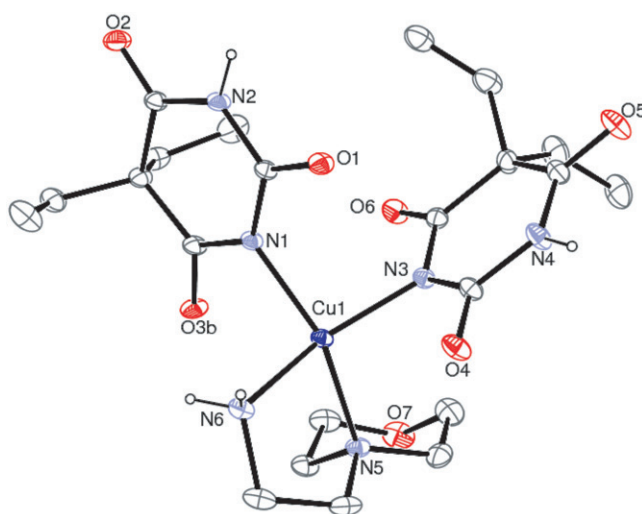
Figure 3.   A molecular view of **3** (C–H hydrogens were omitted for clarity).

Table 3.   Selected bond parameters and hydrogen bonding geometry for **1**.

Bond lengths (Å) and angles (°)			
Cu1–N1	1.992(3)	N3–Cu1–N5	97.83(11)
Cu1–N3	1.986(2)	N5–Cu1–O4	95.20(11)
Cu1–N5	2.078(3)	N6–Cu1–N3	154.88(12)
Cu1–N6	1.982(3)	N6–Cu1–N1	94.05(12)
Cu–O4	2.602(3)	N6–Cu1–N5	85.28(11)
N1–Cu1–N5	149.78(11)	O4–Cu1–N3	56.48(11)
N1–Cu1–O4	114.72(11)	O4–Cu1–N6	98.48(12)
N3–Cu1–N1	95.40(11)		

D–H···A	D–H (Å)	H···A (Å)	D···A (Å)	D–H···A (°)
Hydrogen bonds[a]				
N2–H2···O1^i	0.86	2.06	2.923(4)	176
N4–H4···O5^{ii}	0.86	2.20	3.059(5)	174
N6–H6D···O5^{iii}	0.90	2.62	3.175(4)	121
N6–H6E···O4^{iv}	0.90	2.02	2.864(4)	155
O1W–H1W···O6	0.83(7)	2.37(9)	2.983(5)	131(10)

[a]Symmetry codes: (i) $-x+1, -y+1, -z+1$; (ii) $-x, -y+1, -z+1$; (iii) $x+1/2, y+1/2, z$; (iv) $-x+1/2, -y+3/2, -z+1$.

five coordinate with one aepi or aepyrd and two barb. The structural index parameter τ is a measure of the degree of distortion for pentacoordinate complexes ($\tau = 0$ for an ideal square-pyramid and $\tau = 1$ for an ideal trigonal-bipyramid) [13]. The τ values are 0.09 for **1** and 0.05 for **2**, suggesting distorted square-pyramidal coordination geometry (figures 1 and 2). The N atoms form the basal plane, while oxygen occupies the apical site of the square pyramid. The aepip and aepyrd ligands are bidentate through their nitrogens forming five-membered chelate rings. Complexes **1** and **2** have unequal coordination of barb. One barb is N-coordinated, whereas the other is bidentate through the negatively charged nitrogen and a carbonyl oxygen. Simultaneous presence

Table 4. Selected bond parameters and hydrogen bonding geometry for **2**.

Bond lengths (Å) and angles (°)			
Cu1–N1	1.995(3)	N3–Cu1–N1	95.70(12)
Cu1–N3	1.978(3)	N3–Cu1–N6	154.22(14)
Cu1–N5	2.070(3)	N6–Cu1–N5	84.41(14)
Cu1–N6	1.995(3)	O4–Cu1–N1	116.36(13)
Cu–O4	2.639(3)	O4–Cu1–N3	55.60(13)
N1–Cu1–N5	151.39(15)	O4–Cu1–N5	92.05(14)
N1–Cu1–N6	94.06(13)	O4–Cu1– N6	98.76(14)
N3–Cu1–N5	97.89(13)		

D–H$\cdots$A	D–H (Å)	H$\cdots$A (Å)	D$\cdots$A (Å)	D–H$\cdots$A (°)
Hydrogen bonds[a]				
N2–H2$\cdots$O1[i]	0.86	2.05	2.903(4)	175
N4–H4$\cdots$O5[ii]	0.86	2.13	2.983(5)	174
N6–H6D$\cdots$O4[iii]	0.90	2.04	2.887(4)	157

[a]Symmetry codes: (i) $-x+1$, $-y$, $-z+1$; (ii) $-x+2$, $-y+1$, $-z+1$; (iii) $-x+1$, $-y+1$, $-z+1$.

Table 5. Selected bond parameters and hydrogen bonding geometry for **3**.

Bond lengths (Å) and angles (°)			
Cu1–N1	1.986(3)	N1–Cu1–N6	92.42(12)
Cu1–N3	1.972(3)	N3–Cu1–N5	99.40(12)
Cu1–N5	2.092(3)	N3–Cu1–N1	95.40(11)
Cu1–N6	2.001(3)	N3–Cu1–N6	152.02(14)
N1–Cu1–N5	155.26(12)	N6–Cu1–N5	83.72(12)

D–H$\cdots$A	D–H (Å)	H$\cdots$A (Å)	D$\cdots$A (Å)	D–H$\cdots$A (°)
Hydrogen bonds[a]				
N2–H2$\cdots$O1[i]	0.86	2.07	2.903(4)	175
N4–H4$\cdots$O5[ii]	0.86	2.10	2.951(5)	170
N6–H6D$\cdots$O4[iii]	0.90	2.08	2.902(4)	151

[a]Symmetry codes: (i) $-x+1$, $-y+1$, $-z+1$; (ii) $-x+2$, $-y+2$, $-z+1$; (iii) $-x+2$, $-y+1$, $-z+1$.

of two different coordination modes of barb has not been reported previously. The coordination environment around copper(II) in **3** is square planar with a bidentate aemorph ligand and two monodentate barb anions (figure 3).

The Cu–N$_{barb}$ bond distances in **1**–**3** range from 1.97–2.00 Å, similar to those found in reported barb complexes [10, 14–16]. Compared to the Cu–N bonds, the Cu–O bonds in **1** and **2** are significantly longer, indicating weaker interaction of the carbonyl O with copper(II) as a result of the pseudo Jahn–Teller effect. The Cu–N$_{diamine}$ distances are similar to those of $[(\mu\text{-}1,1,3\text{-}N_3)_2\{Cu_2(L)_2(N_3)_2\}]_n$ [17], $[Cu(L1)(N_3)_2]_n$ [18], and $[CuL_2(Py)(H_2O)](ClO_4) \cdot H_2O$ [19] (L = aepip and L1 = aemrph). A copper(II) complex of aepyrd has not appeared in the literature yet, and **2** is the first copper(II) complex of aepyrd. The six-membered piperidine and morpholine rings in **1** and **3**, respectively, are essentially cyclohexane-like chair conformation. The bond angles in tables 3–5 obviously show distortion in the coordination polyhedra in **1**–**3**. The highest deviation is observed in the bite angle of the barb ligands.

All complexes exhibit interesting intermoleculer hydrogen bonding interactions as listed in tables 3–5. The molecules of **1** are doubly bridged by N–H $\cdots$ O hydrogen bonds involving barb into 1-D zig-zag chains running along the *b* axis; these chains are further linked by water molecules (O–H $\cdots$ O hydrogen bonds) into a 2-D layer parallel to the *b–c* plane. In **2** and **3**, molecules interact through the N–H $\cdots$ O hydrogen bonds between the barb ligands, leading to 1-D zig-zag chains running along the *c* axis.

3.3. *Thermal decomposition studies*

Thermal decomposition behaviors of **1–3** were studied by TGA and DTA in air from 25–900°C. The final decomposition residues were confirmed by mass loss calculations. All three complexes show continuous mass loss from overlapping decomposition of both diamine and barb. However, the position of the exo- or endothermic peaks in the DTA or DTG curves gives an idea for decomposition pathways of these complexes.

Complex **1** dehydrates with a mass loss of 1.4% (Anal. Calcd 1.58%) and dehydrated complex is stable to the melting point observed as a sharp DTA peak centered at 188°C. The endothermic DTA peaks at 256, 261, 271, and 278°C correspond to elimination of aepip and also indicate a complicated degradation process. The highly exothermic peak at 446°C is from decomposition of two barb ligands. Decomposition ends at 487°C to give CuO, with a total mass loss of 86.7% (Anal. Calcd 86.00%). Complex **2** melts at 198°C and has endothermic DTA peaks at 257, 275, 280, and 294°C due to removal of aepyrd, while the violently exothermic DTA peak at 485°C is related to decomposition of barb ligands to give CuO as the final decomposition product (total mass loss: found 85.4% and Anal. Calcd 85.4%) at 494°C. Similarly, **3** shows a continuous mass loss upon heating and endothermic peaks at 238, 274, and 292°C are associated with decomposition of aemrph, whereas the two barb ligands decompose exothermically at 469°C. Overall mass loss is 87.1% (Anal. Calcd 85.80%). The end product at 498°C was CuO.

Supplementary material

Acknowledgement

References

[1] L. Levi, C.E. Hubley. *Anal. Chem.*, **28**, 1591 (1956).
[2] B.C. Wang, B.M. Craven. *Chem. Commun.*, 290 (1971).
[3] L.R. Nassimbeni, A. Rodgers. *Acta Cryst.*, **B30**, 2593 (1974).
[4] M.R. Caira, G.V. Fazakerley, P.W. Linder, L.R. Nassimbeni. *Acta Cryst.*, **B29**, 2898 (1973).
[5] G.V. Fazakerley, P.W. Linder, L.R. Nassimbeni, A.L. Rodgers. *Inorg. Chim. Acta*, **9**, 193 (1974).
[6] L. Nassimbeni, A. Rodgers. *Acta Cryst.*, **B30**, 1953 (1974).
[7] Y. Xiong, C. He, T.C. An, C.H. Cha, X.H. Zhu. *Transition Met. Chem.*, **28**, 69 (2003).
[8] K. Noguchi, H. Yuge, T.K. Miyamato. *Acta Cryst.*, **C56**, e40 (2000).
[9] K. Noguchi, T. Tamura, H. Yuge, T.K. Miyamato. *Acta Cryst.*, **C56**, 171 (2000).
[10] F. Yilmaz, V.T. Yilmaz, C. Kazak. *Z. Anorg. Allg. Chem.*, **631**, 1536 (2005).
[11] V.T. Yilmaz, F. Yilmaz, H. Karakaya, O. Buyukgungor, W.T.A. Harrison. *Polyhedron*, **25**, 2829 (2006).
[12] G.M. Sheldrick. *Acta Cryst.*, **A64**, 112 (2008).
[13] A.W. Addison, T.N. Rao, J. Reedijk, J. van Rijn, G.C. Verschoor. *J. Chem. Soc., Dalton Trans.*, 1349 (1984).
[14] M.R. Caira, G.V. Fazakerley, P.W. Linder, L.R. Nassimbeni. *Acta Cryst.*, **B29**, 2898 (1973).
[15] G.V. Fazakerley, P.W. Linder, L.R. Nassimbeni, A.L. Rodgers. *Cryst. Struct. Commun.*, **3**, 463 (1974).
[16] I.M. Müller, D. Möller. *Eur. J. Inorg. Chem.*, 257 (2005).
[17] T.K. Maji, P.S. Mukherjee, S. Koner, G. Mostafa, J.-P. Tuchagues, N.R. Chaudhuri. *Inorg. Chim. Acta*, **314**, 111 (2001).
[18] Y.S. You, C.S. Hong, K.M. Kim. *Polyhedron*, **24**, 249 (2005).
[19] Y.-G. Li, D.-H. Shi, H.-L. Zhu, H. Yan, S.W. Ng. *Inorg. Chim. Acta*, **360**, 2881 (2007).